ACS APPLIED MATERIALS & INTERFACES

Article

Multifunctional Dumbbell-Shaped DNA-Templated Selective Formation of Fluorescent Silver Nanoclusters or Copper Nanoparticles for Sensitive Detection of Biomolecules

Jinyang Chen, Xinghu Ji, Philip Tinnefeld, and Zhike He

ACS Appl. Mater. Interfaces, **Just Accepted Manuscript** • DOI: 10.1021/acsami.5b09678 • Publication Date (Web): 31 Dec 2015

Just Accepted

ACS Publications

ACS Applied Materials & Interfaces is published by the American Chemical Society.
1155 Sixteenth Street N.W., Washington, DC 20036

Multifunctional Dumbbell-Shaped DNA-Templated Selective Formation of Fluorescent Silver Nanoclusters or Copper Nanoparticles for Sensitive Detection of Biomolecules

Jinyang Chen,[1] Xinghu Ji,[1] Philip Tinnefeld,[2] Zhike He[1,2]*

[1] Key Laboratory of Analytical Chemistry for Biology and Medicine (Ministry of Education), College of Chemistry and Molecular Sciences, Wuhan University, Wuhan 430072, P. R. China

[2] NanoBioSciences Group, Institute for Physical and Theoretical Chemistry and Braunschweig Integrated Centre of Systems Biology (BRICS), and Laboratory for Emerging Nanometrology (LENA), Braunschweig University of Technology, Braunschweig, 38106, Germany

ABSTRACT: In this work, a multifunctional template for selective formation of fluorescent silver nanoclusters (AgNCs) or copper nanoparticles (CuNPs) is put forward. This dumbbell-shaped (DS) DNA template is made up of two cytosine hairpin loops and an adenine-thymine-rich double-helical stem which is closed by the loops. The cytosine loops act as specific regions for the growth of AgNCs, and the double-helical stem serves as template for the CuNPs formation. By carefully investigating the sequence and length of DS DNA, the optimal design of the template is presented. Benefiting from the smart design and facile synthesis, a simple, label-free and ultrasensitive fluorescence strategy for adenosine triphosphate (ATP) detection is proposed. Through the systematic comparison, it is found that the strategy based on CuNPs formation is more sensitive for ATP assay than that based on AgNCs synthesis, and the detection limitation was found to be 81 pM. What's more, the CuNPs formation-based method is successfully applied in the detection of ATP in human serum as well as the determination of cellular ATP. In addition to small target molecule, the sensing strategy was also extended to the detection of biomacromolecule (DNA), which illustrates the generality of this biosensor.

KEYWORDS: multifunctional template; DNA; silver nanocluster; copper nanoparticle; bioassays

1. INTRODUCTION

As promising alternatives for organic dyes and quantum dots, fluorescent nanoclusters or nanoparticles have attracted special research interest due to their unique physical, electrical, and optical properties.[1-5] The template synthesis has been the mainstream approach for fabricating metal nanoclusters or nanoparticles with tunable fluorescence emission and high photostability.[6] By virtue of a unique nanosized linear geometric structure, excellent molecule recognition properties, and high affinity for some metal ions, DNA has been exploited as an important template for mediated synthesis of metal nanomaterials.[7-8] Since they were first reported by Dickson and co-workers,[1] fluorescent silver nanoclusters (AgNCs) stabilized by DNA have attracted increasing interest due to their excellent performance including facile synthesis, easy functionalization, good compatibility, low toxicity and sequence dependence. And the AgNCs have shown great promise for biological labeling,[9] biosensing,[10-14] and information storage.[15] In general, the DNA template used to synthesize brightly fluorescent AgNCs is cytosine-rich sequence or similar single-stranded DNA (ssDNA).[16-18] Besides, there are also studies shown that the single-stranded loop region of hairpin DNA, mismatched double-stranded DNA (dsDNA) or dsDNA with abasic site could serve as the templates for AgNCs synthesis and these strategies were successfully employed to identify single-nucleotide polymorphisms (SNPs).[19-22] As another class of powerfully fluorescent nanomaterials, newly emerging copper nanoparticles (CuNPs), which selectively form on DNA templates, offer excellent potential as novel fluorescent markers. Controlled formation of CuNPs on pre-selected sections of dsDNA has been demonstrated by Mokhir and co-workers.[4] The formed dsDNA-CuNPs exhibited excellent fluorescence properties and proved efficient for biochemical sensing in further studies.[23-25] What's more, Ouyang's group found that, compared with random dsDNA, adenine-thymine (AT)-rich sequences were the better templates for highly fluorescent CuNPs.[26] Recently, Wang and co-workers reported that that

ssDNA also can act as an efficient template for the formation of fluorescent CuNPs.[27] And the selective metallization on ssDNA was achieved in a sequence-specific manner.[28] A high degree of poly-T was essential for the formation of fluorescent CuNPs.

Adenosine-5'-triphosphate (ATP) is a multifunctional nucleotide, which is not only a universal energy source, but also an extracellular signaling mediator and involved in many biological processes, including membrane ion-channel pump, DNA replication, biosynthesis, hormonal and neuronal activities.[29-31] It has also been used as an indicator of living organisms for cell viability and cell injury.[32] Therefore, the highly sensitive and selective detection of ATP is essential for biochemical research as well as clinical diagnosis. Many methods based on host-guest receptors, peptides, conjugated polymers, DNA/RNA aptamers, and ATP-dependent ligation reactions have been developed for ATP detection.[33-39] Among these reported strategies, some of them exhibit only moderate sensitivity with detection limits for ATP in the micromolar or nanomolar range. In addition, even though some methods have shown very good analytical performance, they usually require pre-labeling of a signal source, which needs considerable time-consumption and may suffer from higher cost.

Herein, we designed and put forward a multifunctional template which can not only be used to stabilize fluorescent AgNCs, but also for the formation of CuNPs. This template is a dumbbell-shaped (DS) DNA molecule that consists of a double-helical stem closed by two cytosine hairpin loops. The cytosine loops acted as specific regions for the growth of AgNCs, and the double-helical stem served as template for the CuNPs formation. In order to obtain the optimal template for the synthesis of AgNCs or CuNPs, the DS DNA was carefully designed and investigated by adjusting the length and sequence of DNA. Furthermore, benefiting from the smart design and facile synthesis, a label-free and ultrasensitive fluorescence strategy for ATP detection was presented. Since ATP induced the ligation of the nicking site and sealed the DS DNA which could resist the digestion of exonucleases and then served as the template for the formation of AgNCs or CuNPs, both the fluorescence emission intensity of the AgNCs

and that of CuNPs were used to quantify the ATP concentration. Through the systematic investigation and comparison of the sensitivity of ATP detection based on the AgNCs synthesis and that based on CuNPs formation, it is found that the CuNPs formation-based ATP assay is more sensitive. Moreover, the satisfactory results in the analysis of ATP in human serum as well as the determination of cellular ATP demonstrate that the proposed sensing system possesses great potential for practical application. Additionally, the sensing strategy was also extended to the detection of target DNA, which reveals that the biosensor is capable to detect both small molecule and biomacromolecule.

2. EXPERIMENTAL SECTION

Materials and Reagents: All oligonucleotide with different sequences were synthesized and HPLC purified by Sangon Biotechnology Co., Ltd (Shanghai, China). The sequences of the oligonucleotide used in this work are listed in Table S1 (SI). T4 DNA ligase, Exo I and Exo III were purchased from the Takara Biotechnology Co., Ltd. (Dalian, China). Silver nitrate ($AgNO_3$), sodium borohydride (NaBH4), copper sulfate pentahydrate ($CuSO_4 \cdot 5H_2O$) and ascorbic acid were purchased from Sigma-Aldrich (USA). Shrimp alkaline phosphatase (SAP), Adenosine triphosphate (ATP) and its analogues were obtained from Sigma-Aldrich (USA) as well. Human serum sample was supplied by the Zhongnan Hospital of Wuhan University (Wuhan, China). Cell culture dishes were was obtained from NEST Biotechnology (Beijing, China). Culture medium and fetal bovine serum (FBS) were purchased from Gibco BRL (Grand Island, NY, USA). All chemical reagents were of analytical grade and used without further purification. All solutions were prepared with ultrapure water (18.25 MΩ·cm) from a Millipore system.

Apparatus: Fluorescence spectra were obtained with a RF-5301PC spectrophotometer (Shimadzu, Japan) equipped with a 150 W xenon lamp (Ushio Inc, Japan). UV-vis absorption spectra were recorded by a UV-2250 spectrophotometer (Shimadzu, Japan) using a 1-cm path

length quartz cuvette. Gels were imaged by a ChemiDoc XRD system (Bio-Rad). Transmission electron microscopy (TEM) and high-resolution (HR) TEM images were recorded on a JEOL Ltd. JEM 2100 electron microscope (Japan).

Preparation of AgNCs and CuNPs: The DS DNA was firstly denatured at 95 ºC for 10 minutes followed with a slow annealing treatment for 1 hour before use. For AgNCs synthesis, 50 μL of 2 μM DS DNA was mixed with 250 μL of phosphate buffer (20 mM phosphate, 1 mM magnesium acetate, pH = 7.0), and then 2 μL of 0.6 mM $AgNO_3$ solution was added to the mixture solution. After cooling at 4 ºC for 15 minutes, the mixtures were reduced with 2 μL of 1.2 mM freshly prepared $NaBH_4$, followed by vigorous shaking for 30 seconds. The reaction was kept in the dark at room temperature for 6 hours. For CuNPs synthesis, 50 μL of 2 μM DS DNA was mixed with 250 μL of MOPS buffer (10 mM MOPS, 150 mM NaCl, pH = 7.6), and then 5 μL of 80 mM ascorbic acid was added to the DNA solution. After blending completely, 5 μL of 0.8 mM Cu^{2+} was added and incubated at room temperature to form fluorescent CuNPs within 5 minutes.

Procedures for ATP Assay: In a typical procedure, first, the DS DNA was diluted with 25 mM Tris-HCl buffer (100 mM $NaNO_3$, 6 mM magnesium acetate, pH = 7.6) and denatured at 95 ºC for 10 minutes followed with a slow annealing treatment for 1 hour before use. Then the DS DNA was sealed by adding 1 μL of T4 DNA ligase (350 U/μL) and 5 μL different concentrations of ATP into to the 50 μL of 2 μM DS DNA solution and allowing the ATP-triggered ligation reaction at room temperature for 50 minutes. After that, 4 μL of Exo I (5 U/μL) and 5 μL of Exo III (200 U/μL) were added into the mixture solution to induce the digestion for 60 minutes. The digestion reaction was terminated by incubation at 80 ºC for 5 minutes. Finally, the remaining DS DNA template in the mixture solution was employed to prepare AgNCs or CuNPs with the protocols mentioned above. The time scale of AgNCs

synthesis-based sensing strategy is about 10.5 hours, and that of CuNPs formation-based sensing strategy is about 4.5 hours.

Agarose Gel Electrophoresis: After the ligation and digestion reactions mentioned above, the mixture was stained with 100× SYBR Green I (1 μL). 3 % agarose gel was prepared using 1× TAE buffer (40 mM Tris AcOH, 2 mM Na_2EDTA, pH = 8.5). The electrophoresis was carried out at 100 V for approximately 50 min in 1× TAE buffer. Then the gel was imaged by a ChemiDoc XRD system (Bio-Rad).

Cellular ATP Assay: CAL27 cell is human oral squamous carcinoma cell line obtained from School and Hospital of Stomatology, Wuhan University, China. CAL27 cells were maintained through passaging with 0.25% Trypsin-EDTA three times a week with Dulbecco's Modified Eagle's Medium (DMEM) supplemented with 10% fetal bovine serum (FBS) and 1% penicillin/streptomycin at 37 ºC under 5% CO_2 atmosphere. The collected cells were centrifuged at 3000 rpm for 3 minutes at 4 ºC and washed three times by PBS buffer (20 mM phosphate, 100 mM NaCl, and 5 mM KCl, pH = 7.4) and then suspended in 25 mM Tris-HCl buffer (100 mM $NaNO_3$, 6 mM magnesium acetate, pH = 7.6). Cell lysis was performed by repeated cycles of freezing and thawing, and then the lysed cells were ready for ATP assays. For control experiment, the above CAL27 cell lysate (approximately 100000 cells/mL, 400 μL) was treated with 5 units SAP at 37 ºC for 20 minutes to remove the ATP.

Procedures for DNA Detection: First, the Probe DNA was diluted with 25 mM Tris-HCl buffer (100 mM $NaNO_3$, 6 mM magnesium acetate, pH = 7.6). 25 μL of 4 μM Probe DNA was mixed with 25 μL different concentrations of Target DNA and denatured at 85 ºC for 10 minutes followed with a slow annealing treatment for 1 hour. Then, 1 μL of T4 DNA ligase (350 U/μL) and 5 μL of 800 μM ATP were added into the mixtures and kept at room temperature for 50 minutes. After that, 4 μL of Exo I (5 U/μL) and 5 μL of Exo III (200 U/μL) were added into the mixture solution to induce the digestion for 60 minutes. The

digestion reaction was terminated by incubation at 80 ºC for 5 minutes. Finally, the remaining Probe DNA template in the mixture solution was employed to prepare CuNPs with the protocols mentioned above.

3. RESULTS AND DISCUSSION

3.1. Design of the Multifunctional Template

In the past, many efforts have been made in the DNA-templated metal nanoclusters and nanoparticles. And various DNA templates were explored to individually synthesize AgNCs or CuNPs. Among them, Wang's group found that the duplex DNA scaffold formed by inserting cytosine loop into dsDNA could be used for the generation of fluorescent AgNCs.[20] Mokhir and co-workers reported that dsDNA could be employed as template for the formation of CuNPs.[4] Afterwards, it was proved that the dsDNA-templated CuNPs formation was achieved in a sequence-specific manner.[26] Inspired by these interesting findings, we herein design a multifunctional DNA molecule which can serve as the template not only for the *in situ* AgNCs generation, but also the CuNPs formation. This DS DNA template consists of two cytosine hairpin loops and a double-helical stem which is closed by the loops. The cytosine loops act as specific regions for the growth of AgNCs, and the double-helical stem serves as template for the CuNPs formation.

In order to obtain the optimal fluorescence emission intensities of the AgNCs and CuNPs, the size of cytosine loops and the sequence of the double-helical stem were investigated, respectively. Firstly, the DS DNAs with same double-helical stem closed by cytosine loops with different sizes were explored as the templates to stabilize AgNCs. As shown in Figure 1A, the fluorescence intensity of the AgNCs stabilized by the DS DNA with six-base cytosine (C6) loops is much stronger than that by DNA 1 with C4 loops and DNA 2 with C8 loops. It is indicated that the size of C6 cytosine loops is more suitable for AgNCs formation compared

with that of C4 or C8, and the detailed mechanism and reason is needed to further investigation. So the DS DNA with C6 loops was chosen as the optimal template for the AgNCs synthesis. Secondly, the sequence and length of the double-helical stem of the proposed multifunctional template were evaluated. Comparing the fluorescence intensity of the CuNPs formed in the DS DNA with that in DNA 3, it obviously reveals that the CuNPs formation in the AT-rich double-helical stem is more efficient than that in the double-helical stem with random sequence, which is consistent with previous report (Figure 1B).[26] Moreover, the fluorescence intensity of the CuNPs formed in DNA 4 has no significant change compared with that in DS DNA, even though the double-helical stem of DNA 4 is much longer than that of DS DNA. It is further confirmed that the AT-rich sequences play a dominant role in the dsDNA-templated CuNPs formation against other random sequences. Furthermore, the length of A-T pairs in double-helix stem was evaluated. As shown in Figure 1C, the fluorescence intensity of the formed CuNPs dramatically increased with the increase of the length of A-T pairs range from 16 to 32. It is noted that the enhancement of fluorescence intensity became slow down obviously when the length of A-T pairs reached to 24. Taking into consideration of the enhancement of fluorescence intensity and the cost of DNA, the DS DNA containing 24 A-T pairs in double-helical stem was chosen as the most suitable template for CuNPs formation in this work. Additionally, the spacers with three base pairs were inserted between the loops and the stem.

3.2. Characterizations of Fluorescent AgNCs and CuNPs

In this work, the AgNCs were synthesized through the reduction of $AgNO_3$ with $NaBH_4$ in the presence of DS DNA. And the formation of CuNPs on DS DNA was realized by reducing $CuSO_4$ with ascorbic acid. The as-prepared AgNCs and CuNPs were studied by using fluorescence spectroscopy, UV-vis absorption spectroscopy and transmission electron microscopy (TEM). As shown in Figure 2A, the fluorescence excitation and emission maxima

of AgNCs were at 490 and 573 nm, respectively. And the AgNCs solution was light yellow under daylight and exhibited orange color under UV light. The maximum excitation and emission wavelengths of CuNPs were 343 and 575 nm, respectively (Figure 2B). The CuNPs solution was also bright orange under UV light, but was colorless under daylight. Moreover, the characteristic absorption peaks of AgNCs and CuNPs similar to their excitation spectra appeared in the recorded UV-vis absorption spectrum (Figure 2C, D). The DS DNA-templated formations of AgNCs and CuNPs were also evidenced by the TEM images which clearly showed that the formed AgNCs and CuNPs were spherical in shape, and the average sizes of them were about 1.5 nm and 5.2 nm, respectively (Figure 2E, F). Besides, the obvious crystal lattice structures of AgNCs and CuNPs were presented in the HR TEM images, respectively, which revealed their high crystallinities (Insets of Figure 2E, F). In addition, for the same DS DNA concentration, it is found that the fluorescence intensity of AgNCs was weaker than that of CuNPs (Figure S1, Supporting Information (SI)).

3.3. Principle and Feasibility of ATP Detection

Benefiting from the smart design of the template and the facile synthesis of metal nanomaterials, a simple, label-free and ultrasensitive strategy of ATP assay is developed. The principle of this method is illustrated in Scheme 1, in addition to being a multifunctional template for subsequent AgNCs or CuNPs formation, the unsealed DS DNA also acts as a probe for ATP detection in the sensing system. In the absence of cofactor ATP, the ligation reaction could not be initiated by T4 DNA ligase. So the unsealed DS DNA is digested by Exonuclease III (Exo III) which can degrade the double-helical stem of unsealed DS DNA from the nick, releases 5'-mononucleotides from the 3'-ends of double-helical stem and produces stretches of ssDNA. Then the remaining ssDNA was completely digested by Exonuclease I (Exo I) which can degrade ssDNA from 3'-ends to 5'-ends. After the cyclic digestions by Exo III and Exo I, the unsealed DS DNA was completely degraded as

mononucleotides. Therefore, no template is offered for the preparation of AgNCs or CuNPs, which provides a low background for the sensing system. However, in the presence of ATP, the unsealed DS DNA is sealed and can resist the digestion of Exo I and Exo III due to the T4 ligase-catalyzed ligation reaction. As a result, the selective formation of fluorescent AgNCs or CuNPs within the DS DNA template is realized. Both the fluorescence signal of AgNCs and that of CuNPs could be utilized for the ATP determination.

To demonstrate the feasibility of the proposed strategy, the fluorescence emission spectra of the formed CuNPs under different conditions were investigated. As illustrated in Figure 3A, in the absence of ATP, no obvious fluorescence emission at 575 nm was detected (curve b), which was almost the same as the fluorescence signal in the condition that DS DNA was completely digested by Exo I and Exo III (curve a). It is revealed that this sensing strategy possesses a highly reduced background. This ultra-low background signal is mainly attributed to the efficient digestion of the DS DNA template when the ligation reaction is not triggered. In contrast, a significant fluorescence emission of CuNPs was observed in the presence of 100 nM ATP (curve c). These results suggest that the proposed method is feasible for ATP detection. In order to further confirm the feasibility of the proposed strategy, the experiment of agarose gel electrophoresis was carried out. As shown in Figure 3B, only in the presence of DS DNA, a strong fluorescence band was easily identified (lane 1). The same fluorescence intensity and mobility were observed when DS DNA, ATP and T4 ligase were included but without Exo I and Exo III (lane 2). However, in the presence of DS DNA, T4 ligase and exonucleases, but without ATP, the DS DNA was digested by the exonucleases due to the failed ligation reaction. Consequently, no obvious band was visualized in lane 3. While, in the presence of ATP, the ligation reaction was successfully triggered, so the sealed DS DNA could resist the digestion of exonucleases. As a result, an evident band was observed in lane 4, and the band indicated the same mobility with that in the control experiments (lane 1, 2). The

above results successfully verified that the proposed strategy was entirely feasible for the ATP detection.

3.4. Performance of ATP Detection

In the ATP assay, the digestion procedures of exonucleases play vital roles in the performance of the sensing system, because they are in direct relation to the background signal. So the effects of the exonucleases concentrations and digestion time on the background signal were evaluated first. The optimization experiments were carried out in the absence of ATP, and the exonucleases concentrations and digestion time were defined as optimum value when the background signal reached to the minimum. Through the successive investigations, the optimal concentrations of Exo III and Exo I were 2.5 and 0.05 U/μL, respectively. The digestion time was fixed at 60 min (Figure S2, SI). Besides, as key factors for fluorescence enhancement in the presence of ATP, the T4 ligase concentration and ligation time were optimized as well. The optimal concentration of T4 ligase was 0.875 U/μL, and the optimal ligation time was 50 min (Figure S3, SI). What's more, the influence of Ag^+ concentration on the AgNCs synthesis was investigated. With the increase of Ag^+ concentration, the fluorescence emission intensity increased at first and then gradually decreased after 3 μM (Figure S4, SI). Similarly, the effect of Cu^{2+} concentration on the CuNPs formation was also explored. The result revealed that the fluorescence emission was the most significant when the Cu^{2+} concentration was 100 μM (Figure S5, SI).

Since both the fluorescence signal of AgNCs and that of CuNPs could be utilized for the ATP detection, the sensitivity of AgNCs synthesis-based strategy and that of CuNPs formation-based strategy were investigated, respectively. Under the optimized conditions discussed above, the linear response range of the AgNCs synthesis-based sensing system was measured. As shown in Figure S6 (SI), the fluorescence intensity of AgNCs dramatically increased with the increase of the concentration of ATP, and the fluorescence intensity versus

ATP concentration is plotted at a concentration range (50 ~ 4000 nM). There is a good linear relationship (R^2 = 0.9955) between the fluorescence intensities and the concentrations of ATP with a 28 nM detection limit (signal-to-noise ratio of 3). To our knowledge, this sensitivity exceeds those previously reported fluorescence nanosensing strategies.[38, 40-42] Moreover, the AgNCs formation-based ATP assay broadens the application of fluorescent AgNCs in small molecule detection. The performance of the strategy based on CuNPs formation was also evaluated. As illustrated in Figure 4A and B, the fluorescence intensity of CuNPs gradually increased with the increase of the ATP concentration, and shows a clear linear dependence (R^2 = 0.9938) on the ATP concentration over the range from 0.1 to 125 nM. The limit of detection (LOD) was calculated as 81 pM based on the linear fitting and the noise level of 3 times the standard deviation of a blank solution (n = 11). To the best of our knowledge, this LOD is superior to those of previously reported fluorescence nanosensing systems, and even can be comparable with or exceed those of some previously reported electrochemical strategies (Table S2, SI).[37-46] The high sensitivity is mainly attributed to the ultra-low background signal caused by exonucleases digestions and the strong fluorescence emission of CuNPs. Additionally, due to the larger Stokes shift and shorter time to prepare of CuNPs, the sensing strategy based on CuNPs formation was mainly employed in subsequent analysis and application.

Selectivity is a critical parameter to evaluate the performance of a fluorescence sensing system. Thanks to the high fidelity of the coenzyme dependence of T4 DNA ligase, the strategy possesses inherently high selectivity for ATP detection. In this work, the selectivity of the CuNPs formation-based strategy has been tested by comparing the fluorescence signal of samples containing ATP with those of its analogues, including cytidine triphosphate (CTP), guanosine triphosphate (GTP), uridine triphosphate (UTP), and adenosine diphosphate (ADP). As shown in Figure 4C and D, when ATP, CTP, GTP, UTP and ADP were added to the sensing system, respectively, only ATP caused a marked fluorescence increase. While the

others made no obvious changes in fluorescence intensity, their fluorescence intensities were almost the same as that of the blank solution without ATP, even though the concentration of the analogues was ten times as that of ATP. Therefore, the proposed strategy is capable for ATP assay with a satisfactory selectivity.

3.5. Real Sample Analysis

To challenge the detection toward the target in complex biological matrix, the CuNPs formation-based method was employed to detect ATP in human serum samples. Different concentrations of ATP at 0, 20 nM, 50 nM and 100 nM were separately spiked into the 10% diluted human serum and then the samples were tested with the proposed strategy. As shown in Figure 5A, in the absence of ATP, a relatively high fluorescence background noise was observed in the diluted serum sample. This is mainly due to the matrix effect caused by some proteins present in serum. Nevertheless, in the presence of ATP with different concentrations, the fluorescence signals detected in the diluted human serum had no significant differences with those obtained in buffer. Such satisfactory results were attributed to the procedure of annealing during the interval between the digestion reaction and CuNPs formation, which would inactivate the interfering protein and effectively eliminate the influences of complex matrix on the preparation of CuNPs. It is demonstrated that the ATP assay can be performed in complex biological environment with this sensing strategy. Therefore, the ATP assay in real sample was further carried out through the detection of ATP in cancer cells (CAL27 cells). As illustrated in Figure 5B, in the absence of cell lysates, no obvious fluorescence emission was observed (curve a). However, in the presence of lysates from different numbers of CAL27 cells, all the prominent fluorescence signals were obtained (curve b, c, and d). Furthermore, when the cell lysates were treated with shrimp alkaline phosphatase (SAP) to remove the ATP, almost no significant fluorescence enhancement was observed as anticipated

(curve e). The above results clearly show the robustness of the proposed method in real sample analysis.

3.6. Generality of the Strategy

To illustrate the generality of our design, the DNA detection was carried out through appropriate modification of the sensing strategy. The tumor suppressor genes namely exon segments of p16 chosen as the target model. The principle of DNA detection is shown in Scheme S1 (SI). In the presence of Target DNA, the ligation reaction could not be initiated by T4 DNA ligase due to the hybridization of Probe DNA and Target DNA. So the Probe DNA is digested by Exo I and Exo III and no template is offered for the preparation of CuNPs. In contrary, in the absence of Target DNA, the Probe DNA is sealed and can resist the digestion of exonucleases. Therefore, the fluorescent CuNPs were easily generated and resulted in significant fluorescence response. As shown in Figure S7 (SI), the fluorescence intensity of CuNPs gradually decreased with the increase of the concentration of Target DNA. The plot of the relative fluorescence intensity (ΔF) versus Target DNA concentration is shown in Figure 6A. A good liner relationship (R^2 = 0.9946) could be obtained over the range from 0.1 to 150 nM. Moreover, this method can provide an excellent capability in differentiating between perfectly matched and mismatched DNA targets (Figure 6B).

4. CONCLUSIONS

In summary, a smart and multifunctional DNA template was designed and successfully employed for the selective formation of fluorescent AgNCs or CuNPs. The AgNCs and CuNPs were formed within the different regions of the same template. The systematic characterization and comparison of the same DS DNA-hosted AgNCs and CuNPs confirmed that both the template design and material synthesis were desirable as expected. To the best of our knowledge, this is the first attempt to explore a versatile DNA template which can serve

for the multiple preparations of different metal nanomaterials. What's more, based on the selective *in-situ* formation of AgNCs or CuNPs in the multifunctional template, a simple, label-free and sensitive biosensor for ATP was developed. Thanks to its high sensitivity and selectivity, the sensing strategy was successfully applied in the detection of ATP in real sample, which indicates that the proposed sensing system possesses great potential for practical application. Furthermore, the proposed strategy was also extended in the application of DNA detection, displaying the versatility and generality of our design.

ASSOCIATED CONTENT

Supporting Information

Supplementary tables (Table S1 and S2), supplementary figures (Figure S1 to S7), and Scheme S1. This material is available free of charge via the Internet at http://pubs.acs.org.

AUTHOR INFORMATION

Corresponding Author

*Tel: +86 27-68756557; fax: +86-27-68754067. E-mail: zhkhe@whu.edu.cn.

Notes

The authors declare no competing financial interest.

ACKNOWLEDGMENT

This work was supported by the National Natural Science Foundation of China (21275109, 21205089, 21475101), the Suzhou Nanotechnology Special Project (ZXG2013028), and the Humboldt Foundation for Professor Zhike He.

REFERENCES

(1) Petty, J. T.; Zheng, J.; Hud, N. V.; Dickson, R. M., DNA-Templated Ag Nanocluster Formation. *J. Am. Chem. Soc.* **2004,** *126* (16), 5207-5212.

(2) Richards, C. I.; Choi, S.; Hsiang, J. C.; Antoku, Y.; Vosch, T.; Bongiorno, A.; Tzeng, Y. L.; Dickson, R. M., Oligonucleotide-Stabilized Ag Nanocluster Fluorophores. *J. Am. Chem. Soc.* **2008,** *130* (15), 5038-5039.

(3) Xie, J.; Zheng, Y.; Ying, J. Y., Protein-Directed Synthesis of Highly Fluorescent Gold Nanoclusters. *J. Am. Chem. Soc.* **2009,** *131* (3), 888-889.

(4) Rotaru, A.; Dutta, S.; Jentzsch, E.; Gothelf, K.; Mokhir, A., Selective dsDNA-Templated Formation of Copper Nanoparticles in Solution. *Angew. Chem., Int. Ed.* **2010,** *49* (33), 5665-5667.

(5) Tanaka, S.; Miyazaki, J.; Tiwari, D. K.; Jin, T.; Inouye, Y., Fluorescent Platinum Nanoclusters: Synthesis, Purification, Characterization, and Application to Bioimaging. *Angew. Chem., Int. Ed.* **2011,** *50* (2), 431-435.

(6) Kumar, A.; Kumar, V., Biotemplated Inorganic Nanostructures: Supramolecular Directed Nanosystems of Semiconductor(s)/Metal(s) Mediated by Nucleic Acids and Their Properties. *Chem. Rev.* **2014,** *114* (14), 7044-7078.

(7) Yeh, H. C.; Sharma, J.; Han, J. J.; Martinez, J. S.; Werner, J. H., A DNA-Silver Nanocluster Probe That Fluoresces Upon Hybridization. *Nano Lett.* **2010,** *10* (8), 3106-3110.

(8) Zhang, L.; Zhu, J.; Zhou, Z.; Guo, S.; Li, J.; Dong, S.; Wang, E., A New Approach to Light up DNA/Ag Nanocluster-Based Beacons for Bioanalysis. *Chem. Sci.* **2013,** *4* (10), 4004.

(9) Yu, J.; Choi, S.; Dickson, R. M., Shuttle-Based Fluorogenic Silver-Cluster Biolabels. *Angew. Chem., Int. Ed.* **2009,** *48* (2), 318-320.

(10) Enkin, N.; Wang, F.; Sharon, E.; Albada, H. B.; Willner, I., Multiplexed Analysis of Genes Using Nucleic Acid-Stabilized Silver-Nanocluster Quantum Dots. *ACS Nano* **2014,** *8* (11), 11666-11673.

(11) Zhang, Y.; Zhu, C.; Zhang, L.; Tan, C.; Yang, J.; Chen, B.; Wang, L.; Zhang, H., DNA-Templated Silver Nanoclusters for Multiplexed Fluorescent DNA Detection. *Small* **2015,** *11* (12), 1385-1389.

(12) Liu, X.; Wang, F.; Aizen, R.; Yehezkeli, O.; Willner, I., Graphene Oxide/Nucleic-Acid-Stabilized Silver Nanoclusters: Functional Hybrid Materials for Optical Aptamer Sensing and Multiplexed Analysis of Pathogenic Dnas. *J. Am. Chem. Soc.* **2013,** *135* (32), 11832-11839.

(13) Zhang, L.; Zhu, J.; Guo, S.; Li, T.; Li, J.; Wang, E., Photoinduced Electron Transfer of DNA/Ag Nanoclusters Modulated by G-Quadruplex/Hemin Complex for the Construction of Versatile Biosensors. *J. Am. Chem. Soc.* **2013,** *135* (7), 2403-2406.

(14) Zhang, L.; Zhao, J.; Duan, M.; Zhang, H.; Jiang, J.; Yu, R., Inhibition of dsDNA-Templated Copper Nanoparticles by Pyrophosphate as a Label-Free Fluorescent Strategy for Alkaline Phosphatase Assay. *Anal. Chem.* **2013,** *85* (8), 3797-3801.

(15) Huang, Z.; Tao, Y.; Pu, F.; Ren, J.; Qu, X., Versatile Logic Devices Based on Programmable

DNA-Regulated Silver-Nanocluster Signal Transducers. *Chem. - Eur. J.* **2012,** *18* (21), 6663-6669.

(16) Sharma, J.; Rocha, R. C.; Phipps, M. L.; Yeh, H. C.; Balatsky, K. A.; Vu, D. M.; Shreve, A. P.; Werner, J. H.; Martinez, J. S., A DNA-Templated Fluorescent Silver Nanocluster with Enhanced Stability. *Nanoscale* **2012,** *4* (14), 4107-4110.

(17) Sharma, J.; Yeh, H. C.; Yoo, H.; Werner, J. H.; Martinez, J. S., A Complementary Palette of Fluorescent Silver Nanoclusters. *Chem. Commun.* **2010,** *46* (19), 3280-3282.

(18) Obliosca, J. M.; Babin, M. C.; Liu, C.; Liu, Y. L.; Chen, Y. A.; Batson, R. A.; Ganguly, M.; Petty, J. T.; Yeh, H. C., A Complementary Palette of Nanocluster Beacons. *ACS Nano* **2014,** *8* (10), 10150-10160.

(19) Gwinn, E. G.; O'Neill, P.; Guerrero, A. J.; Bouwmeester, D.; Fygenson, D. K., Sequence-Dependent Fluorescence of DNA-Hosted Silver Nanoclusters. *Adv. Mater.* **2008,** *20* (2), 279-283.

(20) Guo, W.; Yuan, J.; Dong, Q.; Wang, E., Highly Sequence-Dependent Formation of Fluorescent Silver Nanoclusters in Hybridized DNA Duplexes for Single Nucleotide Mutation Identification. *J. Am. Chem. Soc.* **2010,** *132* (3), 932-934.

(21) Huang, Z.; Pu, F.; Hu, D.; Wang, C.; Ren, J.; Qu, X., Site-Specific DNA-Programmed Growth of Fluorescent and Functional Silver Nanoclusters. *Chem. - Eur. J.* **2011,** *17* (13), 3774-3780.

(22) Kun, M.; Qinghua, C.; Guiying, L.; Fei, W.; Shujuan, X.; Yong, S., DNA Abasic Site-Directed Formation of Fluorescent Silver Nanoclusters for Selective Nucleobase Recognition. *Nanotechnology* **2011,** *22* (30), 305502.

(23) Jia, X.; Li, J.; Han, L.; Ren, J.; Yang, X.; Wang, E., DNA-Hosted Copper Nanoclusters for Fluorescent Identification of Single Nucleotide Polymorphisms. *ACS Nano* **2012,** *6* (4), 3311-3317.

(24) Chen, J.; Liu, J.; Fang, Z.; Zeng, L., Random dsDNA-Templated Formation of Copper Nanoparticles as Novel Fluorescence Probes for Label-Free Lead Ions Detection. *Chem. Commun.* **2012,** *48* (7), 1057-1059.

(25) Qing, Z.; Qing, T.; Mao, Z.; He, X.; Wang, K.; Zou, Z.; Shi, H.; He, D., dsDNA-Specific Fluorescent Copper Nanoparticles as a "Green" Nano-Dye for Polymerization-Mediated Biochemical Analysis. *Chem. Commun.* **2014,** *50* (84), 12746-12748.

(26) Song, Q.; Shi, Y.; He, D.; Xu, S.; Ouyang, J., Sequence-Dependent dsDNA-Templated Formation of Fluorescent Copper Nanoparticles. *Chem. - Eur. J.* **2015,** *21* (6), 2417-2422.

(27) Qing, Z.; He, X.; He, D.; Wang, K.; Xu, F.; Qing, T.; Yang, X., Poly(Thymine)-Templated Selective Formation of Fluorescent Copper Nanoparticles. *Angew. Chem., Int. Ed.* **2013,** *52* (37), 9719-9722.

(28) Guiying, L.; Yong, S.; Jian, P.; Wei, D.; Lingling, L.; Shujuan, X.; Fei, W.; Xiaohua, W., Highly Thymine-Dependent Formation of Fluorescent Copper Nanoparticles Templated by ss-DNA. *Nanotechnology* **2013,** *24* (34), 345502.

(29) Szewczyk, A.; Pikuła, S. a., Adenosine 5′-Triphosphate: An Intracellular Metabolic Messenger. *Biochim. Biophys. Acta* **1998,** *1365* (3), 333-353.

(30) Abraham, E. H.; Okunieff, P.; Scala, S.; Vos, P.; Oosterveld, M. J.; Chen, A. Y.; Shrivastav, B., Cystic Fibrosis Transmembrane Conductance Regulator and Adenosine Triphosphate. *Science* **1997,** *275* (5304), 1324-1326.

(31) Newman, E. A.; Zahs, K. R., Calcium Waves in Retinal Glial Cells. *Science* **1997,** *275* (5301), 844-847.

(32) Eguchi, Y.; Shimizu, S.; Tsujimoto, Y., Intracellular ATP Levels Determine Cell Death Fate by Apoptosis or Necrosis. *Cancer Res.* **1997,** *57* (10), 1835-1840.

(33) Mizukami, S.; Nagano, T.; Urano, Y.; Odani, A.; Kikuchi, K., A Fluorescent Anion Sensor That Works in Neutral Aqueous Solution for Bioanalytical Application. *J. Am. Chem. Soc.* **2002,** *124* (15), 3920-3925.

(34) McCleskey, S. C.; Griffin, M. J.; Schneider, S. E.; McDevitt, J. T.; Anslyn, E. V., Differential Receptors Create Patterns Diagnostic for ATP and GTP. *J. Am. Chem. Soc.* **2003,** *125* (5), 1114-1115.

(35) Li, C.; Numata, M.; Takeuchi, M.; Shinkai, S., A Sensitive Colorimetric and Fluorescent Probe Based on a Polythiophene Derivative for the Detection of ATP. *Angew. Chem., Int. Ed.* **2005,** *44* (39), 6371-6374.

(36) Lin, C.; Cai, Z.; Wang, Y.; Zhu, Z.; Yang, C. J.; Chen, X., Label-Free Fluorescence Strategy for Sensitive Detection of Adenosine Triphosphate Using a Loop DNA Probe with Low Background Noise. *Anal. Chem.* **2014,** *86* (14), 6758-6762.

(37) Zhou, Z.; Du, Y.; Dong, S., Double-Strand DNA-Templated Formation of Copper Nanoparticles as Fluorescent Probe for Label-Free Aptamer Sensor. *Anal. Chem.* **2011,** *83* (13), 5122-5127.

(38) Lu, C. H.; Li, J. A.; Lin, M. H.; Wang, Y. W.; Yang, H. H.; Chen, X.; Chen, G. N., Amplified Aptamer-Based Assay through Catalytic Recycling of the Analyte. *Angew. Chem. Int. Ed.* **2010,** *49* (45), 8454-8457.

(39) Lu, L. M.; Zhang, X. B.; Kong, R. M.; Yang, B.; Tan, W., A Ligation-Triggered Dnazyme Cascade for Amplified Fluorescence Detection of Biological Small Molecules with Zero-Background Signal. *J. Am. Chem. Soc.* **2011,** *133* (30), 11686-11691.

(40) Lu, L.; Qian, Y.; Wang, L.; Ma, K.; Zhang, Y., Metal-Enhanced Fluorescence-Based Core-Shell Ag@SiO_2 Nanoflares for Affinity Biosensing Via Target-Induced Structure Switching of Aptamer. *ACS Appl. Mater. Interfaces* **2014,** *6* (3), 1944-1950.

(41) Liu, C.; Wang, Z.; Jia, H.; Li, Z., Efficient Fluorescence Resonance Energy Transfer between Upconversion Nanophosphors and Graphene Oxide: A Highly Sensitive Biosensing Platform. *Chem. Commun.* **2011,** *47* (16), 4661-4663.

(42) He, Y.; Wang, Z. G.; Tang, H. W.; Pang, D. W., Low Background Signal Platform for the Detection of ATP: When a Molecular Aptamer Beacon Meets Graphene Oxide. *Biosens. Bioelectron.* **2011,** *29* (1), 76-81.

(43) Zhu, W. P.; Zhao, Z. W.; Li, Z.; Li, H.; Jiang, J. H.; Shen, G. L.; Yu, R. Q., A Label Free

Exonuclease III-Aided Fluorescence Assay for Adenosine Triphosphate Based on Graphene Oxide and Ligation Reaction. *New J. Chem.* **2013,** *37* (4), 927-932.

(44) Du, Y.; Li, B.; Wei, H.; Wang, Y.; Wang, E., Multifunctional Label-Free Electrochemical Biosensor Based on an Integrated Aptamer. *Anal. Chem.* **2008,** *80* (13), 5110-5117.

(45) Zhang, H. F.; Han, Y. J.; Guo, Y. J.; Dong, C., Porphyrin Functionalized Graphene Nanosheets-Based Electrochemical Aptasensor for Label-Free ATP Detection. *J. Mater. Chem.* **2012,** *22* (45), 23900-23905.

(46) Lu, L.; Si, J. C.; Gao, Z. F.; Zhang, Y.; Lei, J. L.; Luo, H. Q.; Li, N. B., Highly Selective and Sensitive Electrochemical Biosensor for DNA Based on the Dual Strategy Integrating the Cofactor-Dependent Enzymatic Ligation Reaction with Self-Cleaving Dnazyme-Amplified Electrochemical Detection. *Biosens. Bioelectron.* **2015,** *63* (0), 14-20.

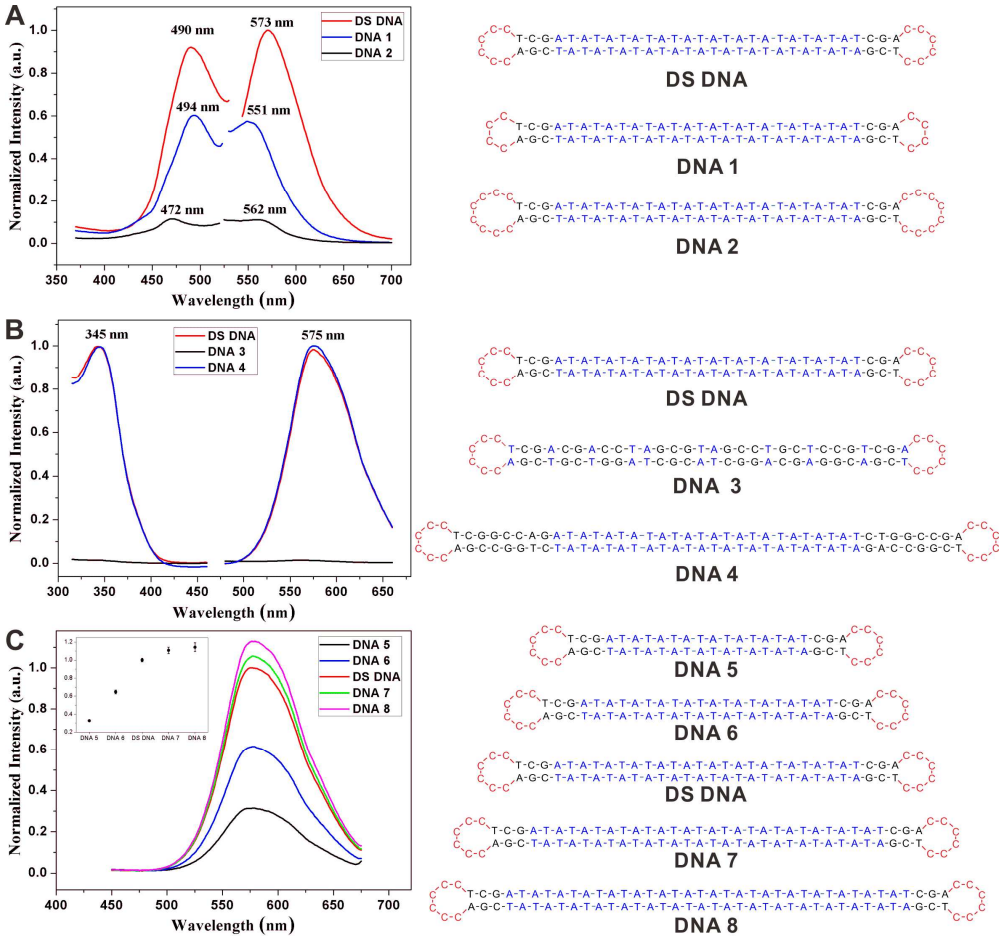

Figure 1. (A) Fluorescence excitation and emission spectra of AgNCs stabilized by the DS DNA, DNA 1 and DNA 2, respectively. (B) Fluorescence excitation and emission spectra of CuNPs formed with the templates of DS DNA, DNA 3 and DNA 4, respectively. (C) Fluorescence emission spectra of CuNPs formed with the templates of DNA 5, DNA 6, DS DNA, DNA 7 and DNA 8, respectively. Inset: the normalized fluorescence intensities of CuNPs with different DNA templates. The designs of corresponding DNA templates are illustrated in right.

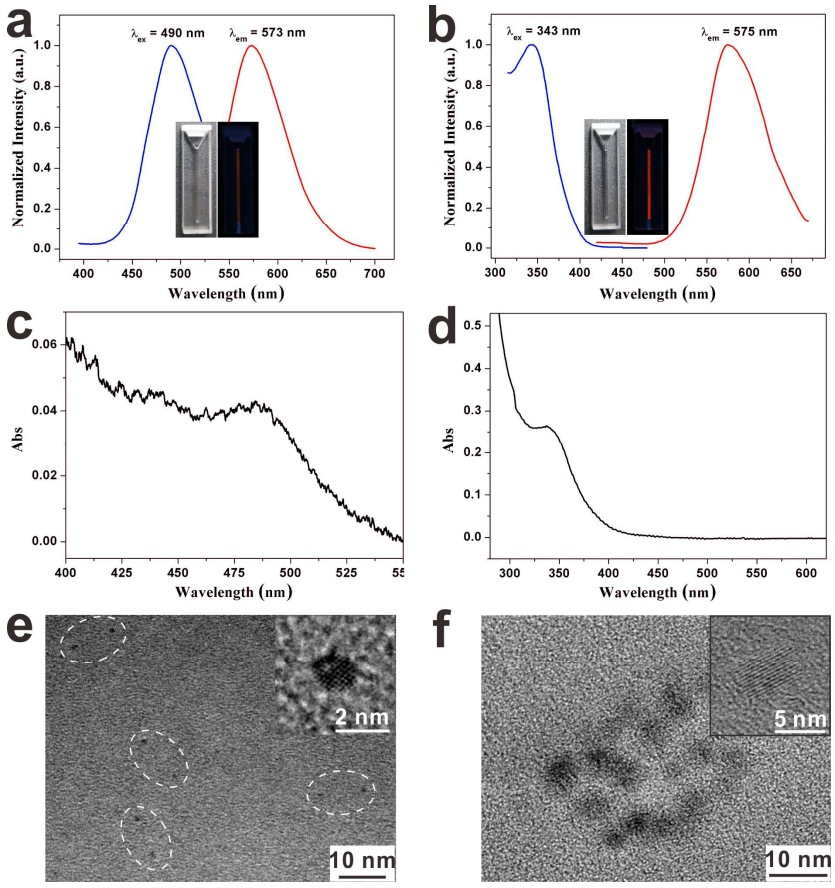

Figure 2. (A) Fluorescence excitation (λ_{ex} = 490 nm) and emission (λ_{em} = 573 nm) spectra of DS DNA-templated AgNCs. (B) Fluorescence excitation (λ_{ex} = 343 nm) and emission (λ_{em} = 575 nm) spectra of DS DNA-templated CuNPs. The insets are the photographs of AgNCs and CuNPs under irradiation with daylight (left) and UV light (right), respectively. UV-vis absorption spectra of DS DNA-templated AgNCs (C) and CuNPs (D). TEM images of DS DNA-templated AgNCs (E) and CuNPs (F). The insets are the HR-TEM images of AgNCs and CuNPs, respectively.

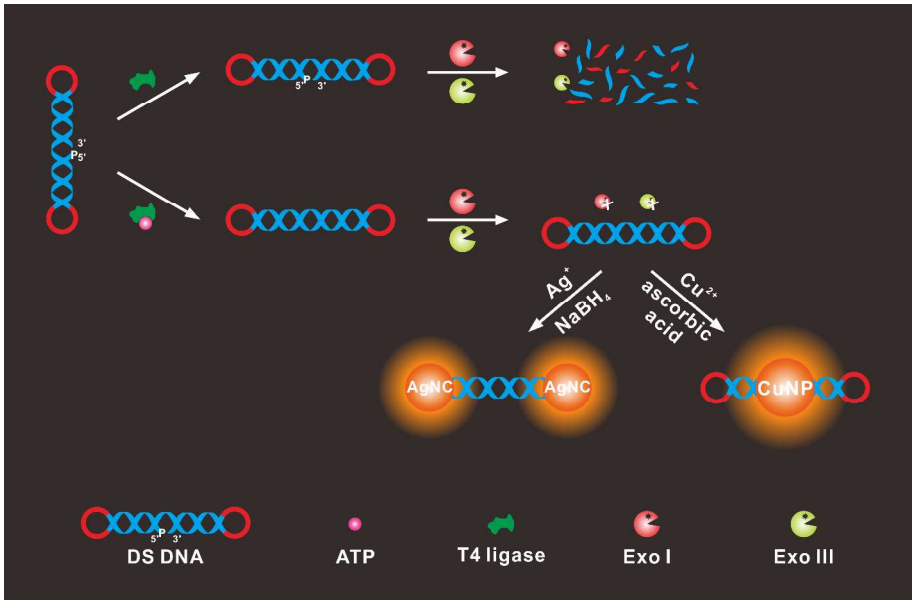

Scheme 1. Schematic illustration of the mechanism for the sensitive detection of ATP based on selective formation of fluorescent AgNCs or CuNPs in DS DNA.

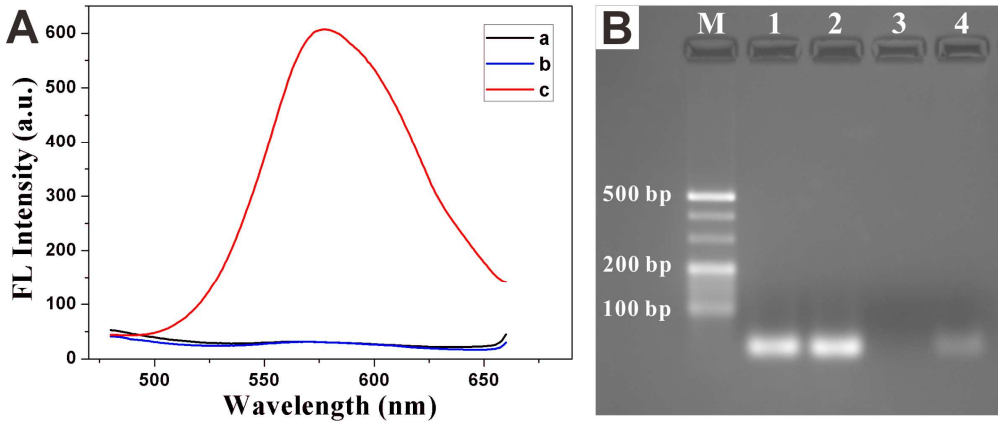

Figure 3. (A) Fluorescence emission spectra of formed CuNPs under different conditions: (a) DS DNA + Exo I + Exo III; (b) DS DNA + T4 ligase + Exo I + Exo III; (c) DS DNA + 100 nM ATP + T4 ligase + Exo I + Exo III. (B) Agarose gel electrophoresis of the products of different experiments. Lane M: DNA ladder; lane 1: DS DNA; lane 2: DS DNA + 100 nM ATP + T4 ligase; lane 3: DS DNA + T4 ligase + Exo I + Exo III; lane 4: DS DNA + 100 nM ATP + T4 ligase + Exo I + Exo III. Concentration of DS DNA was 250 nM.

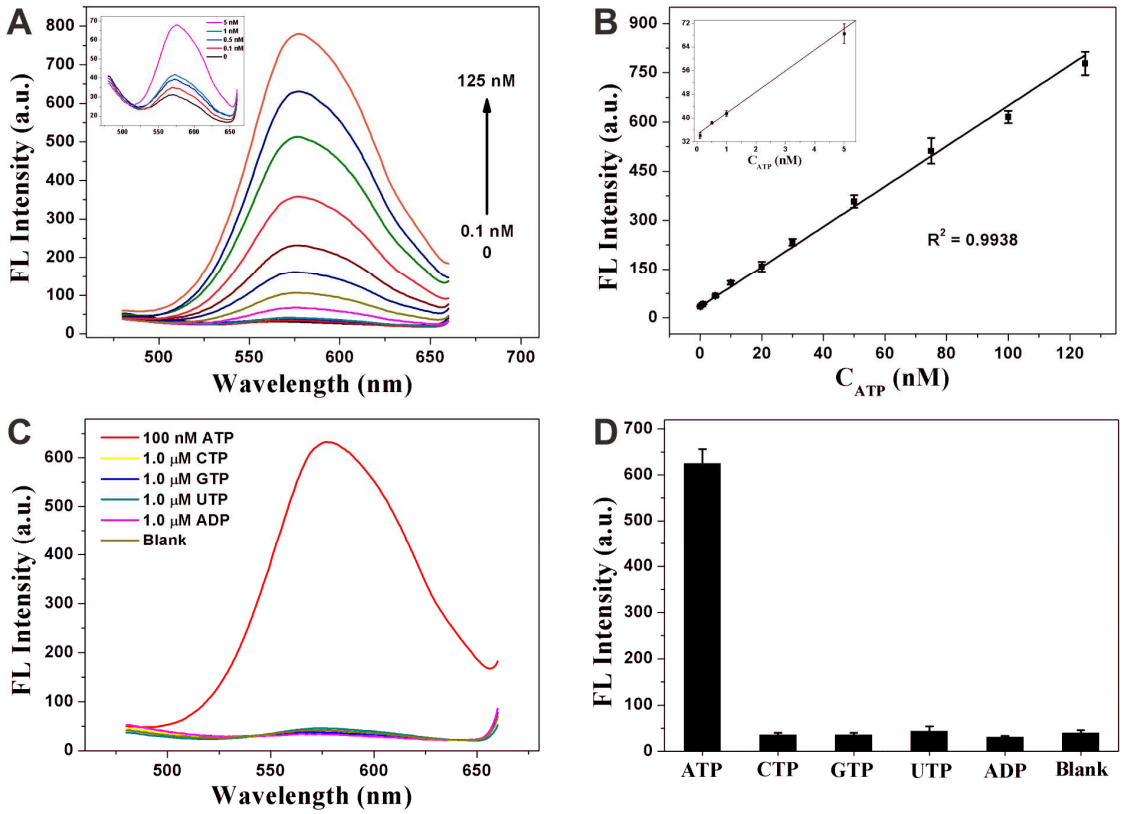

Figure 4. (A) Fluorescence responses of formed CuNPs to the different concentrations of ATP. Inset: Enlarged view of fluorescence responses at low concentrations of ATP. (B) Corresponding calibration curve for ATP detection. Inset: Enlarged view of linear curve at low ATP concentrations. (C), (D) Selectivity of the developed sensing platform for ATP compared to ATP analogues and blank. The concentration of ATP is 100 nM, while the concentrations of CTP, GTP, UTP, and ADP are 1 μM, respectively. The error bars represent the standard deviations based on three parallel measurements.

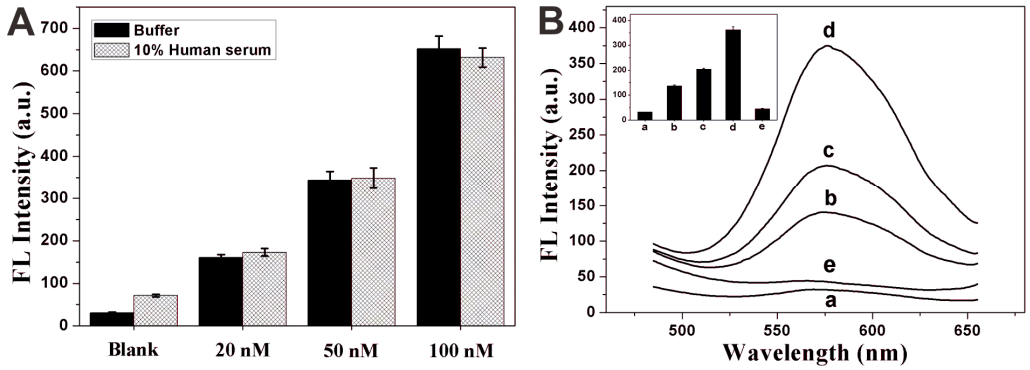

Figure 5. (A) Fluorescence responses of the sensing platform for ATP detection in buffer and 10% diluted human serum samples, respectively. The error bars represent the standard deviations based on three parallel measurements. (B) Fluorescence responses of formed CuNPs in the absence of freshly lysed cells (a), and in the presence of freshly lysed cells with different concentrations: approximately 50000 cells/mL (b), 100000 cells/mL (c), 250000 cells/mL (d), as well as in the presence of SAP-treated lysed cells (100000 cells/mL) (e).

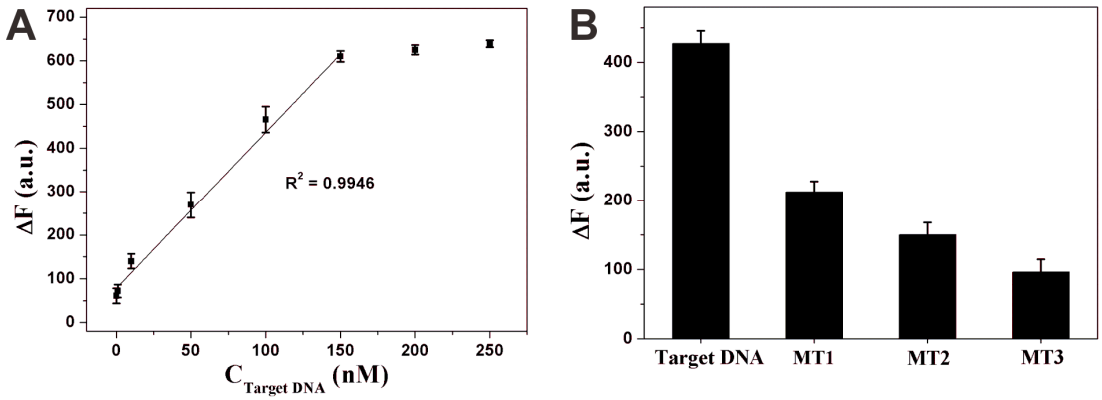

Figure 6. (A) Relationships between relative fluorescence intensities and the concentrations of Target DNA. (B) Fluorescence responses of formed CuNPs in the presence of Target DNA, single-base mismatched target DNA (MT1), two-base mismatched target DNA (MT2) and three-mismatched target DNA (MT3). The error bars represent the standard deviations based on three parallel measurements.

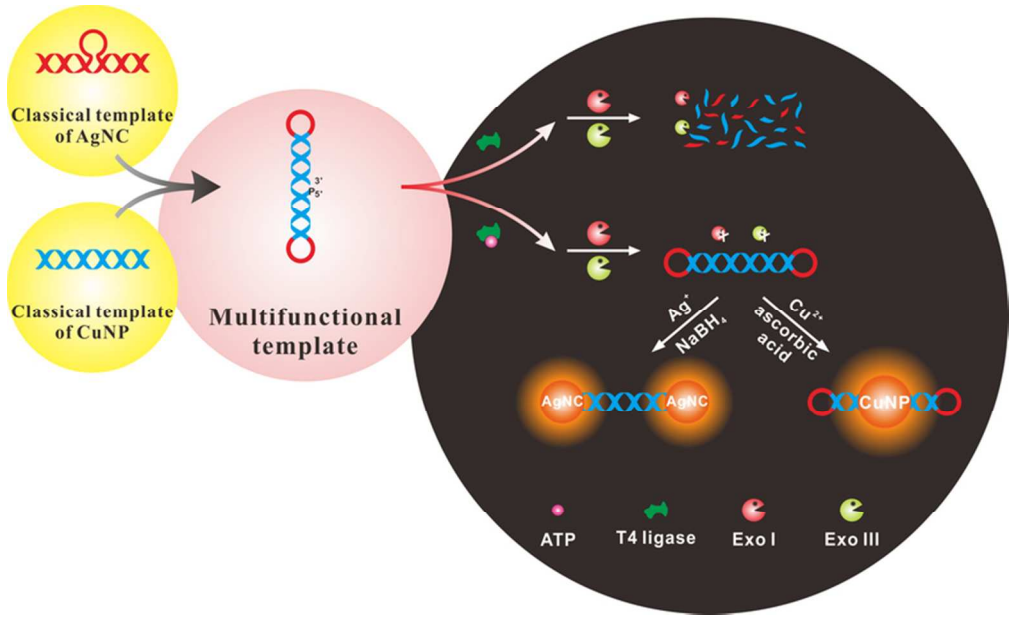

Graphical Abstract
73x44mm (300 x 300 DPI)